Charge on the move: how electron-transfer dynamics depend on molecular conformation

Andrew C. Benniston* and Anthony Harriman

Received 20th September 2005
First published as an Advance Article on the web 30th November 2005
DOI: 10.1039/b503169a

This *tutorial review* illustrates the many facets whereby the molecular conformation helps to control the rates of through-bond electron transfer. A brief introduction to Marcus theory is given, highlighting the importance of the coupling element and the super-exchange mechanism, before considering the reasons why the coupling element might depend on the molecular geometry. The methods currently available for determination of both the coupling element and the geometry are reviewed and various examples are given for systems where the structure controls the degree of electronic coupling along the molecular axis. The role of the "bridge" connecting the donor and acceptor is emphasized.

1. Introduction

A comprehensive understanding of electron-transfer processes is essential for future progress in many diverse fields of science, spanning from biological enzymes to organic synthesis to optoelectronic devices.[1] Over the past few decades, many artificial mimics have been developed to probe electron-transfer events. These systems generally comprise electron donor and acceptor subunits connected *via* an organic bridge. The connector has the dual role of providing structural support for the electrode-active terminals and functioning as a conduit for the rapid and efficient transfer of electronic information at the molecular level. Many different bridges have been proposed for use in conjunction with through-bond electron transfer or exchange. The flux of information along such molecular arrays shows an exquisite dependence on the chemical nature, especially the connectivity, of the bridge. Since it is inconceivable that long bridges might be constructed in any way other than by the accretion of pre-designed building blocks, the key element for the engineering of effective bridges is to control the level of orbital overlap between adjacent subunits. This generic effect can be illustrated by considering the degree of electronic coupling along a poly(phenylene)-based molecular wire. Rapid transfer is predicted for the case where all the rings are aligned in a coplanar geometry but transfer will be seriously impaired if several rings are held in a mutually orthogonal orientation.[2] Being able to modulate the orientation on demand provides for a molecular-scale dimmer switch that could regulate the flow of information along the wire. Here, we review this area

Molecular Photonics Laboratory, School of Natural Sciences, Bedson Building, University of Newcastle, Newcastle upon Tyne, UK NE1 7RU, UK. E-mail: a.c.benniston@ncl.ac.uk; Fax: (0191) 222 8660; Tel: (0191) 222 5706

Dr Andrew C. Benniston

Dr Andrew C. Benniston obtained a PhD from Warwick University in 1991 before receiving a one-year Royal Society Fellowship to work with Dr Jean-Pierre Sauvage at the Université Louis Pasteur in Strasbourg. To extend the scope of this work, Dr Benniston went to work for 3 years with Prof. Harriman in Texas on the synthesis and photochemistry of multi-component supermolecules. Dr. Benniston was appointed to a lectureship at Glasgow University in 1995, where he set up an independent research group. He moved to the University of Newcastle in 2001 and was promoted to a Senior Lectureship in 2003. He is Co-Director of the Molecular Photonics Laboratory, and has published more than 60 research articles.

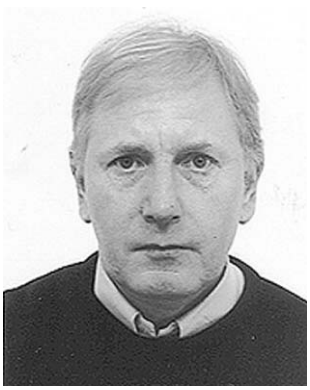

Professor Anthony Harriman

Professor Anthony Harriman spent 14 years at the Royal Institution of Great Britain, where he was Dewar Research Fellow and Assistant Director of the Davy–Faraday Research Laboratory. His main research theme during this period related to artificial photosynthesis. He moved to the University of Texas at Austin in 1988 to become Director of the Center for Fast Kinetics Research. He moved to the Department of Chemistry at the University of Newcastle in October 1999 and was appointed Head of Department in April 2000. His main research interest still involves the design and study of systems intended to mimic natural photosynthesis but is moving progressively towards the emerging field of molecular opto-electronics. He has published more than 320 research articles.

of electron-transfer chemistry and comment on the feasibility of using an orientation switch[3] to control through-bond electron transfer.

2. Marcus theory and beyond

Marcus theory[4] provides the essential basis by which to relate the rate constant for intramolecular electron transfer (k_{ET}) with thermodynamic parameters. Although it has many important limitations, classical Marcus theory is a good starting point for the logical design of donor–acceptor pairs and for understanding the electron-transfer dynamics in terms of molecular structure. The main features are covered in eqn (1)–(3), where λ is the total reorganisation energy, V_{DA} is the electronic coupling matrix element and ΔG° is the change in Gibbs free energy accompanying electron transfer. A key aspect of Marcus theory is the change in free energy of activation $\Delta G^{\#}$ and its parabolic dependence on ΔG° and λ. Eqn (2) indicates that the rate will be activationless when $\Delta G^{\circ} = -\lambda$; a situation that can be reached rather easily by synthetic control. It can be seen from eqn (3) that V_{DA} is predicted to decrease exponentially with increasing separation (d) of donor and acceptor, at least when there is a continuous medium between the reactants.[5] This allows definition of an attenuation factor β that represents the conductivity of the bridging medium and of the coupling element at orbital contact V_0. The reorganisation energy contains contributions from both nuclear and solvent terms and can vary over a very wide range. Again, this permits optimisation of the rate by balancing the reorganisation energy with the thermodynamic driving force.

$$k_{ET} = \frac{2\pi}{\hbar}\frac{|V_{DA}|^2}{\sqrt{4\pi k_B T \lambda}}\exp\left(-\frac{\Delta G^{\#}}{k_B T}\right) \quad (1)$$

$$\Delta G^{\#} = \frac{(\Delta G^0 + \lambda)^2}{4\lambda} \quad (2)$$

$$V_{DA} = V_0 \exp(-\beta d) \quad (3)$$

All the important predictions of classical Marcus theory have been verified by experiment and, under varying conditions, the rate can be satisfactorily described in terms of eqn (1). This includes the so-called "inverted" region where k_{ET} decreases with increasing reaction exoergonicity. Experimental verification has been obtained for each of the three major categories of electron transfer; namely, charge separation, charge recombination and charge shift.[6] Parallel studies have led to the development of quantum chemical approaches to the calculation of λ and V_{DA} and to the screening of putative molecular-scale bridges for effective long-range electron transfer. The past decade has witnessed great and sustained activity in the study of how k_{ET} depends on the chemical composition of the donor–acceptor dyad and especially on the role of the bridge. The key factor is the coupling element and the rational design of advanced molecular dyads requires an improved knowledge of how to control V_{DA} at the molecular level.

3. Super-exchange and electronic coupling

In order to exert proper control over the rate of electron transfer it seems appropriate to insist on intramolecular events and to employ a through-bond mechanism. Here, electron transfer from donor to acceptor proceeds by way of "virtual" orbitals localised on the bridge, even though the bridge does not figure as a real intermediate in the electron-transfer process. Thus, electron transfer uses the bridge LUMO whilst hole transfer borrows electrons from the HOMO of the bridge (Fig. 1). Such a simplistic view involves several gross assumptions, notable that the donor, bridge and acceptor are well defined species whose molecular orbitals can be separated and that the bridge provides a continuous surface for electron/hole transfer. Nonetheless, this crude mechanism, usually termed as "super-exchange",[7] gives important insight into the dynamics of long-range electron transfer in molecular dyads.

$$V_{DA} = \frac{\alpha_{DB}\alpha_{BA}}{\Delta E_{DB}} \quad (4)$$

$$\langle V_{DA}^2 \rangle = \frac{1}{N}\sum_{i=1}^{N}\left(V_{DA}^{(i)}\right)^2 \quad (5)$$

The most important aspect of super-exchange theory is that the coupling element is related to the energy gap (ΔE_{DB}) between active orbitals on the donor and on the bridge (eqn (4)).[8] A large energy gap translates to weak electronic coupling and therefore a slow rate of electron transfer. For a given donor, ΔE_{DB} is determined by the electronic properties of the bridge and considerable research has gone into identifying bridges with high electronic conductivity. The best materials seem to be poly(aromatics), diethynylated aromatics and diethenylated aromatics. Also important in determining the size of V_{DA} are the atomic orbital coefficients that describe coupling between the donor and first member of the bridge (α_{DB}) and between the last member of the bridge and the acceptor (α_{BA}). These latter terms can vary significantly with the site at which the bridge is attached and with the substitution pattern of the donor and/or acceptor.

According to eqn (3), k_{ET} will decrease rather sharply with increasing separation of the reactants and this situation has been confirmed by experiment. However, recent studies have shown several cases where the fall-off in rate is much less than

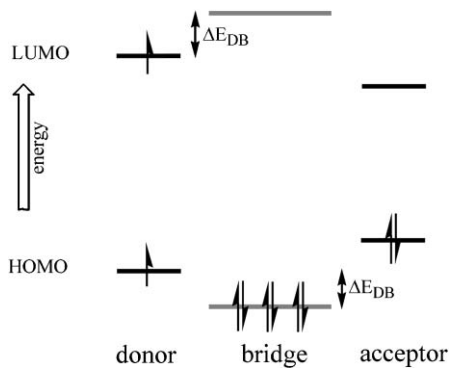

Fig. 1 Pictorial representation of the super-exchange mechanism for electron transfer in a donor–bridge–acceptor dyad.

anticipated.[9–11] In certain examples, the coefficient β seems to vary with the length of the bridge or with solvent polarity. Such cases have been interpreted in terms of a switch in the electron-transfer mechanism from long-range to sequential (or hopping) mechanisms. The latter occurs when components in the bridge act as real redox intermediates. Here, long-range electron transfer is achieved by way of a cascade of short-range steps, each occurring by way of super-exchange (Fig. 2). Both mechanisms can operate simultaneously, their relative importance depending on the experimental conditions.[12] The cascade mechanism usually provides for the faster overall rate but can become incoherent when a series of identical bridging units is employed.

An additional complication for mechanistic studies is that the bridge rarely functions as a single electronic entity. Thus, a metallic conductor has a well-defined resistivity that increases in proportion to its length. Molecular conductors comprise a series of discrete orbitals that offer a disparate level of resistivity. The net effect is a discontinuous conduit with regions of high and low conductivity. A more appropriate description of the coupling element, therefore, is given as eqn (5).[13] Here, $V_{DA}^{(i)}$ is an effective coupling element for the i-th residue in the bridge and N is the total number of units that combine to form the bridge. An individual residue could be a discrete molecular fragment or a particular conformation of a subunit. This approach has been especially useful for the computation of coupling elements for large proteins and has led to clarification of preferred electron-transfer pathways in metallo-enzymes.[14]

4. Quantum mechanical effects and nuclear tunnelling

Numerous experimental studies have shown that the activation energies for electron-transfer processes occurring in the Marcus inverted region ($\Delta G^\circ < -\lambda$) are often substantially less than those predicted on the basis of eqn 2. This effect has been attributed to some of the excess thermal energy being transferred to intramolecular vibrational modes ($h\omega$) associated with the donor or acceptor. The net effect is to lower $\Delta G^\#$ by an amount corresponding to a certain number of quanta of energy $h\omega$. This is a particular issue for charge recombination between highly energetic species and serves to limit the lifetime of charge-separated states. A semi-classical version of the theory, that is easy to use and gives good fits to temperature dependent kinetic data, has been developed by McConnell[15] (eqn (6) and (7)) and is based on the inclusion of a single medium-frequency vibrational mode ($h\omega_M$).

$$k_{ET} = \frac{2\pi}{\hbar}\frac{V_{DA}^2}{\sqrt{2\pi\sigma^2}}\exp\left(-\frac{(\Delta G^0+\lambda)^2}{2\sigma^2}\right) \quad (6)$$

$$\sigma^2 = \lambda h\omega_M \coth\left(\frac{h\omega_M}{2k_B T}\right) \quad (7)$$

A further problem for understanding the rates of electron transfer in the inverted region is that nuclear tunnelling can make an important contribution, especially at low temperature. This has the effect of by-passing the normal transition state, since the electron can tunnel through a narrow barrier. Nuclear tunnelling is especially important for donor–acceptor pairs held in close proximity and where one particular vibrational mode plays a key role. The main effect of nuclear tunnelling is that k_{ET} becomes independent of temperature. It has to be stressed, however, that the rate constant for electron transfer occurring *via* nuclear tunnelling is relatively low.

5. Geometric control of the coupling element

The fact that the magnitude of V_{DA} depends on the nature of the bridge offers the possibility to control the rate of through-bond electron transfer by structural means. One of the key factors relating to the overall electronic resistivity of a putative bridge is how well molecular orbitals on adjacent subunits blend together to form a continuous medium. Thus, the orientation provides one method by which to influence k_{ET} for molecular dyads. Several experimental and theoretical studies have addressed this issue, although the experimental work is hampered by the difficulty to produce systematic series of dyads in which the only variable is the orientation of the bridge. A promising approach was introduced by McLendon *et al.*[16] whereby 4,4′-biphenyl was used as the bridge for two porphyrin termini and the dihedral angle between the phenyl rings was varied by substitution at the 2,2′-positions. It was observed that the rate of through-bond electron transfer was dependent on the angle around the central biphenyl linkage and reached a minimum at 45°. Unfortunately, the substitution pattern also leads to changes in the electronic properties of the bridge, which themselves can affect the size of k_{ET}.

A more rational approach[17] is to attach a tethering strap across the 2,2′-positions, thereby keeping a constant substitution pattern, and using the strap length to control the central torsion angle (Fig. 3). Here, the electronic coupling element can be described in terms of eqn (8) where α_1 and α_2, respectively, refer to coupling between the donor and the bridge and the acceptor and the bridge whilst δ refers to coupling between the adjacent phenyl rings (eqn (8) and (9)). This latter term can be related to the torsion angle ϕ by

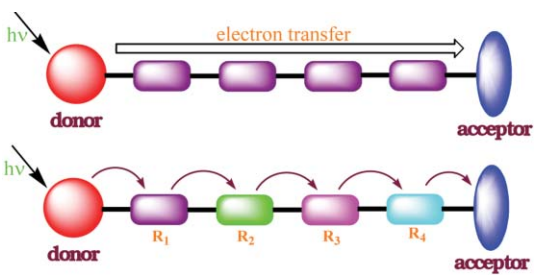

Fig. 2 Comparison of long-range (coherent) and sequential (incoherent) electron-transfer processes.

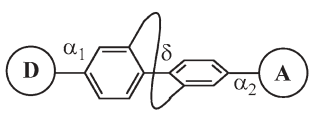

Fig. 3 Tethered strap approach to systematic variation of the central torsion angle.

reference to coupling at 0° (δ_0). A range of torsion angles becomes possible according to the number of carbon atoms in the strap, although thermal fluctuation has to be taken into account. Freezing the sample in a low temperature glassy matrix solves this particular problem. Furthermore, extra oxygen atoms can be built into the strap so as to form the corresponding crown ether.

$$V_{DA} = \frac{\alpha_1 \alpha_2}{\delta} \left| \frac{-\delta}{\Delta_{DB}} \right|^2 \quad (8)$$

$$\delta = \delta_0 (\cos\phi)^2 \quad (9)$$

Coordination of cations inside the central void serves to rigidify the crown and impose a restricted torsion angle around the central biphenyl group (Fig. 4). Thus, a considerable variety of angles can be achieved without serious perturbation of the electronic properties. The effect of torsion angle on the electronic coupling matrix element can then be assessed. It should be emphasized, however, that this approach leads to a distribution of angles at ambient temperature due to thermal motions, as indicated by molecular dynamics simulations.[17] These internal motions can be dampened at low temperature or on solidifying the surrounding matrix.

6. Experimental approaches to V_{DA}

Several methods are available by which to measure the magnitude of V_{DA} for certain molecular dyads. A particularly attractive experimental approach involves recording optical absorption spectra for mixed-valence binuclear complexes formed by selective oxidation of one metallo-terminal.[18] The mixed-valence complex usually exhibits a weak charge-transfer transition in the near IR due to charge hopping between the two terminals *via* super-exchange interactions. For the symmetrical complexes, $\Delta G^\circ = 0$ and V_{DA} can be calculated directly from eqn (10). Here, ε_{MAX} is the molar absorption coefficient at the peak maximum, ν_{MAX} is the absorption maximum in cm^{-1} and FWHM is the full-width at half

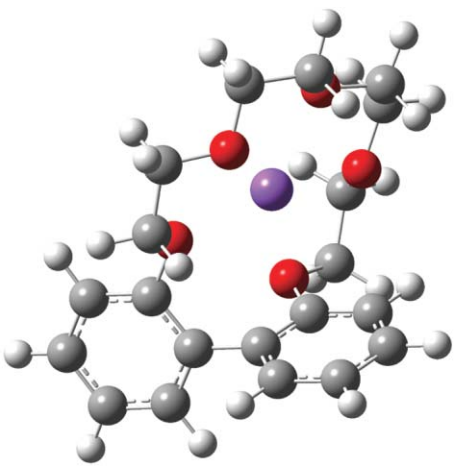

Fig. 4 Energy-minimised structure for a cation-bound complex where the dihedral angle can be changed by complexation. Coordination of a cation into the central crown ether void can be used as a strategy for tightening the torsion angle.

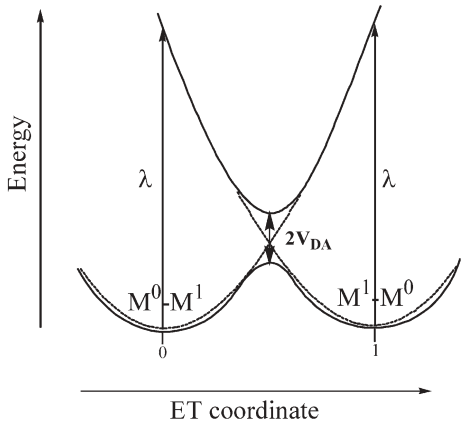

Fig. 5 Potential energy diagram for intervalence charge transfer in symmetrical binuclear complexes.

maximum of the Gaussian-shaped absorption band. The charge-transfer length d is usually taken as the distance between the metal centres, although this might be an over-estimate.[19] This approach, which allows for easy calculation of both the reorganisation energy and the activation energy (Fig. 5), has been highly successful, especially for establishing how V_{DA} depends on separation distance.[20]

$$V_{DA} = \frac{0.0205 \nu_{MAX}}{d} \sqrt{\frac{\varepsilon_{MAX} FWHM}{\nu_{MAX}}} \quad (10)$$

Benniston *et al.*[18] have used the intervalence methodology to measure how torsion angle affects V_{DA} in a series of mixed-valence ruthenium(II/III) bis(2,2′:6′,2″-terpyridine) complexes of the type shown in Fig. 3. Maximal coupling was found at 0° and there was a clear minimum at 90° (Fig. 6). Coupling did not vanish at 90°, however, because of thermal fluctuations about the mean angle. This system represents the first systematic attempt to study the angle dependence without complications from competing variations in the electronic properties of the bridge.

These symmetrical systems are ideal for testing the validity of electron-transfer parameters derived from analysis of their absorption spectral bands, thereby allowing comparison of the calculated rate constant with the experimental value. Unfortunately, it is extremely difficult to extract kinetic information from such measurements since there are no

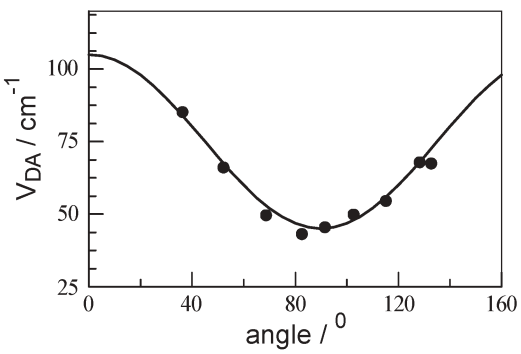

Fig. 6 Effect on torsion angle on the size of the electronic coupling matrix element.

obvious absorption spectral changes upon illumination. This precludes the use of fast laser kinetic measurements relying on optical changes. An alternative approach is to use organic analogues that form stable radical cations and to follow the course of reaction by EPR spectroscopy. Several such studies have been undertaken and show that, within reasonable limits, the theory allows a good estimate of the rate of intramolecular electron transfer, without the need for explicit nuclear tunnelling corrections.

The corresponding binuclear ruthenium(II) complexes show weak phosphorescence in deoxygenated solution at ambient temperature.[21] Upon cooling to 77 K, the emission yield increases markedly since thermal population of higher-lying excited states is curtailed. This allows determination of the rate constant (k_{NR}) for non-radiative decay of the lowest-energy, metal-to-ligand, charge transfer (MLCT) excited triplet state. It was found that k_{NR} depends on torsion angle, with the maximum rate being found at *ca.* 40°. This unexpected effect might be attributed to changes in the degree of electron delocalisation at the triplet level. Thus, illumination of the metal complex results in rapid ejection of an electron from the metal centre to the LUMO localised on the substituted terpyridine ligand (Fig. 7). Because of π-electron conjugation, the promoted electron can sample a sizeable fraction of the bridging ligand but the central biphenyl group presents a barrier to full electron delocalisation. The results suggest that the torsion angle controls the electron distribution at the π-radical anion stage.[21] Similar results are apparent for the corresponding ligand-to-metal, charge transfer transition found for the binuclear ruthenium(III) complexes.

Intramolecular triplet energy transfer takes place in the binuclear mixed-metal complexes possessing ruthenium(II) and osmium(II) terminals. The primary mechanism for such processes involves Dexter-type electron exchange. This is a through-bond interaction involving simultaneous transfer of an electron (through the bridging LUMO) and a positive hole (through the bridging HOMO). The rate constant for electron exchange (k_{EX}) is given by eqn (11). Here, the Franck–Condon weighted density of states (FCWD) can be calculated precisely from emission spectra recorded for donor and acceptor species. As such, the coupling element can be derived directly from kinetic data.

$$k_{EX} = \frac{2\pi}{\hbar}|V_{DA}|^2 \mathrm{FCWD} \qquad (11)$$

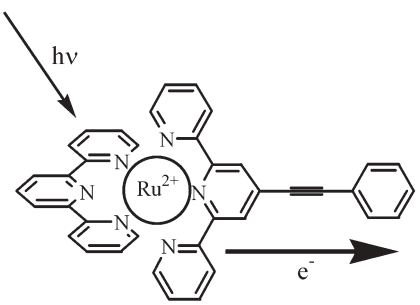

Fig. 7 Pictorial representation of light-induced charge transfer in a substituted metal complex.

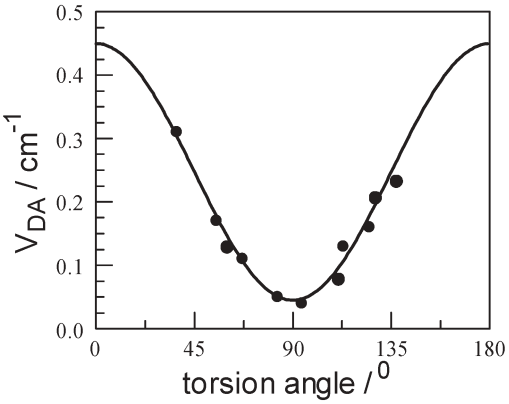

Fig. 8 Effect of torsion angle on the coupling element for electron exchange in the mixed-metal, binuclear complexes.

Benniston *et al.*[22] have used this approach to explore triplet energy transfer in the mixed-metal complexes relating to Fig. 3. Rates are fairly fast, even at 77 K where the molecular geometry is frozen into the lowest-energy conformation. This allows the effect of torsion angle to be evaluated over a wide range of geometries. Again, the results show that the maximum coupling occurs when the biphenyl group is coplanar (Fig. 8). There is a substantial decrease in V_{DA} as the torsion angle increases and a definite minimum around 90°. That the coupling element does not decrease to zero for orthogonal geometries is attributed to nuclear tunnelling across the connecting bond. It is notable that the variation in k_{EX} reaches 80-fold as the angle increases from 0 to 90°. This is clear indication that angular effects are sufficiently pronounced to control the rate of electron exchange.

The same approach can be used to measure rates of intramolecular electron transfer but the FCWD factor is more difficult to calculate. The best approach is to measure the activation energy for electron transfer and thereby expose the rate of electron transfer under activationless conditions. Provided ΔG° is known, the activation energy allows derivation of λ so that V_{DA} can be obtained from kinetic measurements. This is a rather tedious procedure but is the only reliable way to determine V_{DA}. To date, systematic studies have not been applied to the problem of how variations in torsion angle affect V_{DA} for electron transfer.

Other experimental methods, such as EPR, fluorescence spectroscopy or cyclic voltammetry, can be used to measure the extent of electronic communication along the molecular axis. Such approaches are useful but do not allow derivation of V_{DA}. Quantum chemical methods are advancing rapidly, however, and now appear to give reliable estimates of V_{DA} for certain dyads.

7. How to measure molecular conformation

The more complex a molecular system, the greater becomes the difficulty to obtain a meaningful picture of how all the components are arranged, interact, move and behave in solution. As an example, for the simple molecule biphenyl the gas-phase structure reveals the rings to be twisted with a dihedral angle of about 45°. In contrast, the crystal structure

shows the biphenyl molecule to be almost planar. It is accepted that the structure of biphenyl is governed by two competing factors: the drive towards planarity so as to maximise π-conjugation and ortho, ortho′ H–H′ repulsive steric interactions that force the rings to twist. The solid-state structure has the additional problem of crystal packing that tends to drive the molecule to become planar. Evidently, as a structure becomes more multi-component, one could ask the question: does an X-ray structure give a real indication of how the molecule looks in solution or in a semi-fluid phase? This question is somewhat difficult to answer since one must look at the specific compound under study, the different molecular components and their structural flexibility. In the end, the specific information required for a particular compound will be the deciding factor. For example, if the distance between two units separated by a very rigid spacer is required then an X-ray structure (if it can be obtained!) is ideal, whereas calculation of the angle between flexible rings must be done by different methods. Some of these approaches are discussed below.

7.1 NMR spectroscopy

Nuclear magnetic resonance (NMR) spectroscopy is certainly one of the most powerful techniques for obtaining structural information for a compound in fluid solution. Ignoring the obvious compound identification, there are a number of parameters or experiments that afford invaluable insight into molecular structure. It is not the intention here to give an in-depth description of all available NMR techniques since any modern textbook on NMR spectroscopy covers these adequately.

In addition to the chemical shifts of a particular nucleus, scalar coupling constants (*i.e.*, Fermi coupling ($^{n}J_{XY}$)) give some indication of how nuclear spins interact through the valence electrons. The most noteworthy relationship is that given by the Karplus expression (eqn (12)), which relates through-bond coupling to the dihedral angle (Fig. 9). As the measurement of *J* values is rather straightforward it is possible to use these data to acquire insight into dihedral angles. The correlation is especially useful for structures based on cyclopentanes, cyclohexanes, carbohydrates and polycyclic systems.

$$^{3}J_{XY} = A\cos^2(\phi) + B\cos(\phi) + C \qquad (12)$$

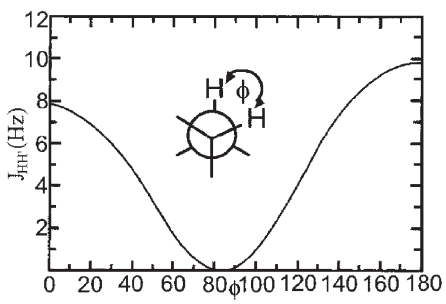

Fig. 9 A typical example of the vicinal Karplus relationship between the dihedral angle (ϕ) and the coupling constant *J*.

Whereas coupling constants can afford some indication of the dihedral angle, the nuclear Overhauser effect (NOE) measures how much of the dipolar relaxation of a given proton occurs *via* cross relaxation with some specific proton. The result contains information on the relative distances between protons in a molecule, and hence constitutes a qualitative measurement of the distance between subunits. The cross relaxation rates depend critically on distance with the effect decreasing according to a reciprocal r^6 dependence. Under normal operating conditions, a measurable effect between ^{1}H nuclei can be expected up to *ca.* 4 Å. Evidently, NOE measurements within complex structures can indicate whether or not molecular components are in close proximity. This knowledge is extremely important as it can often rationalise why electron-transfer events between particular units are fast, how electronic coupling between components occurs, or when charge migration can take place over large distances.

As well as static information, NMR also offers the possibility to gain useful data about chemical or conformational exchange. In fluid solution, a measured spectrum of a compound is in fact the result of fast conformational averaging; coupling constants and NOEs of multi-conformational populations are seen as averages. However, if a molecule is undergoing a dynamic process with a rate constant k (s^{-1}), and this is comparable with the difference in chemical shifts between the individual signals of the exchanging species, then the lines become broad and merge (coalescence). Individual spectra are observed when k is low, and exchange between the species can be studied by techniques such as saturation transfer or EXCSY (Exchange Correlated Spectroscopy). Because NMR is a relatively slow technique, whereas electron-transfer events are often fast, a compound undergoing conformational exchange will be essentially 'frozen' during electron transfer. However, information on the dynamic behaviour is still essential, since rates of electron transfer do not have to be the same for the different conformers.

The technique of NMR is not, of course, only tied to solution phase studies, and in particular solid-state ^{13}C NMR spectroscopy has been widely used to obtain structural information. Whereas in solution molecules tumble rapidly and the chemical shift of a ^{13}C nucleus is isotropic, the same is not true in the solid state. In this case, the chemical shift is anisotropic and the mathematical entity that describes its orientation dependence is called a tensor. Chemical shift tensors (CST) give a handle on structural information and in particular about conformations. Returning to the problem of biphenyl, Grant *et al.*[23] using CST in the solid state were able to show that the internal twist angle between the rings is 15°, with a mean libration angle of $\pm 12°$.

7.2 Resonance raman spectroscopy

Raman techniques have found wide applications for deducing the ground-state conformations of biologically relevant species, such as peptides and visual pigments. For example, in peptides the molecular vibrations act as probes for the local environment, and afford invaluable information on how the

structures fold and unfold. When studying systems that support electron transfer it is often the case that information is required on the excited-state structure, and in particular how the molecular fragments respond (*e.g.*, twist, bend, compress) to a change in charge distribution. For this purpose, time-resolved resonance Raman (TR^3) spectroscopy spanning nanosecond to sub-picosecond time scales has been extremely valuable. A compound that has been studied widely by such techniques is 4-dimethylaminobenzonitrile (DMABN), and many attempts have been made to unequivocally identify its excited-state structure.[24] Although it is not the intention of this article to cover the area of twisted intramolecular charge-transfer (TICT) states, other reviews give an insight into how difficult it can be to completely identify these structures in rotameric molecules such as DMABN.[25,26]

7.3 Molecular modelling

One of the more widely applied methods for collecting structural information is by computer molecular modelling. The extremely high speed and large memory of modern computers, coupled to the wide range of easy-to-handle programs, has opened this field to more and more non-specialists. There is no longer the necessity to laboriously enter coordinates of a molecular structure into a program, as modern modelling systems have a simple graphical interface package that allows one to visualise the target compound. Depending on the level of information required, the acquisition of structural data can take from a few minutes to several weeks to collect.

There are two basic types of molecular modelling: molecular mechanics and quantum mechanics. The first is a classical mechanical model that represents a molecule as a group of atoms held together by elastic bonds; simply put, bonds are like springs which can be stretched, compressed, bent to various angles and twisted into assorted torsion angles. A force field is generated by the sum of all the different force constants. In a molecular mechanics calculation, a force field is chosen and appropriate molecular structure values (*i.e.*, natural bond lengths, angles) are set. The structure is optimised to minimise the strain energy so that the 'minimum energy' structure is obtained. Molecular mechanics is a fast and easily carried out calculation, but suffers from important limitations.

In comparison, quantum mechanics calculations take longer to carry out and rely on solving the Schrödinger equation ($H\psi = E\psi$). The operator H (Hamiltonian) depends on the kinetic and potential energies of electrons and nuclei in a molecule. The wave-function (ψ) affords information on the probability of finding electrons in certain places around a molecule. The term E is related to the energies of individual electrons. To solve the equation for a complex molecule is clearly challenging, but the Born–Oppenheimer approximation and independent electron approximations help alleviate the problem to some extent. Even so, solving the numerous integrals associated with the Schrödinger equation is difficult and time consuming. Two different approaches are possible; namely, *ab initio* methods where all integrals are solved without making approximations and semi-empirical methods (*e.g.*, PM3, AM1) in which parameters are introduced from molecular data, so that integrals can be either ignored or approximated. The former is more suited to small molecules whereas the latter is better for large molecules. More recently, however, the use of density functional theory (DFT) to solve structural problems has come to the fore. The basic theorems of DFT originate from the 1960s, in which the wave-functions associated with the solutions of the Schrödinger equation are replaced by endeavours to calculate an electron density function $\rho(r)$. The determination of such a parameter uniquely defines the ground-state structure of a many-electron molecular system. Indeed DFT calculations can be used to give a complete picture of a molecule in its ground state.

7.4 Molecular dynamics simulations

Molecular dynamics simulations (MDS) augment the molecular mechanics computations by applying fixed amounts of thermal energy. This allows variations in bond angles and lengths to be mapped with respect to time, such that conformational heterogeneity can be probed. In fact, MDS studies are essential if meaningful dynamic structures are to be obtained. Even molecules with constrained geometries undergo considerable structural fluctuation in solution and this has to be accounted for when considering how geometry affects the rate of electron transfer. Thus, consider the strapped biphenyl-based cyclophane that binds small cations in the central void (Fig. 4). MDS studies indicate that the closest approach between the cation and the biphenyl group is subject to considerable variation. The central torsion angle changes accordingly. Clearly, this dynamic behaviour has to be incorporated into the reaction model.

A further illustration of the power of MDS is provided by the aza crown ether linked to a ruthenium(II) tris(2,2′-bipyridyl) complex (Fig. 10).[27] Here, electron transfer between the triplet state of the metal complex and the aza N atom occurs only in those conformations that bring the reactants into close proximity. The structure is rigidified on binding a cation to the crown void. This prevents adoption of the desired conformations and has the effect of switching-off the electron-transfer event.

8. Charge transfer across orthogonal geometries

Theoretical studies[28] made with molecular dyads able to undergo intramolecular charge-shift reactions (Fig. 11) have shown that there is strong electronic coupling between donor and acceptor over a wide range of torsion angles. The initial and final states appear as reasonably well localised species and there is no evidence for TICT formation. Even so, the coupling element becomes rather small for orthogonal geometries. On this basis, it is interesting to note that several experimental studies have described fast electron transfer across orthogonal geometries when the reactants are held in close proximity. Thus, rapid charge separation has been observed in a porphyrin–pyromellitic diimide dyad (Fig. 12).[29] Here, the rate of charge separation was found to be *ca.* 2 ps at room temperature in a mixture of CH_2Cl_2 and pyridine. However, charge recombination occurs with a lifetime of 15 ps so that the ground-state system is restored very quickly. In this case,

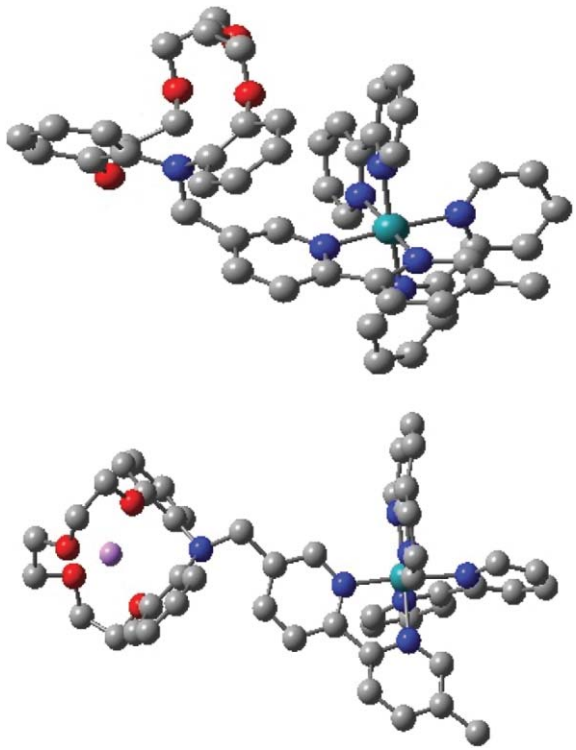

Fig. 10 MDS structures derived for a functionalised crown ether (upper panel) and the corresponding cation complex (lower panel).

there is no temporal resolution of forward and reverse electron-transfer steps to be gained from the orthogonal geometry. Interestingly, inserting a phenyl ring between the reactants has the effect of slowing down charge separation, the mean lifetime being 22 ps, but speeding up charge recombination, the mean lifetime being *ca.* 3 ps. A novel feature of this work relates to the use of time-resolved infrared spectroscopy to follow the course of reaction.[29] Fast light-induced charge shift, occurring over a few ps, has been observed for two 9-aryl-10-methylacridinium cations, although the rates of the corresponding reverse reactions are reported to occur on surprisingly different time scales. Whereas the 9-(2-naphthyl) derivative[30] undergoes reverse charge shift and triplet state formation during a few ns, the charge-shift state formed from the closely related 9-mesityl derivative[31] has a reported lifetime in excess of 2 h at 200 K.

In an attempt to ascertain the influence of conformational changes that occur after intramolecular charge transfer, the

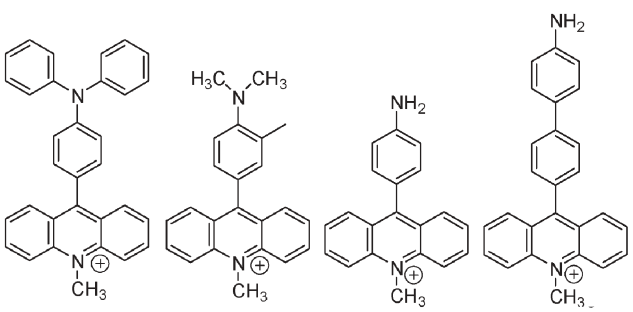

Fig. 11 Examples of donor-substituted *N*-methylacridinium ions used to study charge-shift reactions.

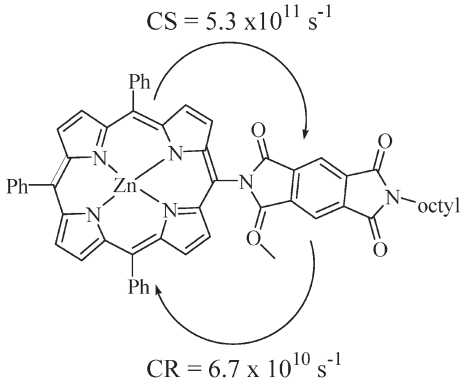

Fig. 12 Porphyrin-pyromellitic diimide dyad displaying an orthogonal geometry but fast rates of forward and reverse electron transfer.

series of compounds **4–6** was studied[32] (Fig. 13). The ground state dihedral angle decreases for these compounds in the order **4 > 5 > 6**. Illumination leads to charge transfer from the *N*,*N*-dimethylaniline to the cyanobenzene unit and to an increased dipole moment along the molecular axis. Reformation of the ground state by reverse electron transfer is accompanied by charge-transfer fluorescence; for all the compounds, and independent of the angle, emission takes place from a singlet charge-transfer state, ^{1}CT. For both the geometrically restricted derivative **6** and the flexible dyad **5**, the radiative rate constant (k_f) displays a weak dependence on solvent polarity. It is contingent from this finding that the emissive state for **5** is planar because of the similarity of the k_f values (35–61 $\times$ 10^7 s^{-1}). In marked contrast, the strongly twisted dyad **4** shows comparable behaviour to **5** and **6** only in non-polar solvents, indicating partial excited state relaxation towards planarity. As the solvent polarity increases, the values of k_f decrease sharply to a minimum value of 3 $\times$ 10^7 s^{-1}. To account for these observations, Rettig and Lapouyade have concluded that the ^{1}CT state for **4** exists as an equilibrium mixture of planar and twisted rotamers.[32]

9. Constrained molecular assemblies

Porphyrins are the natural pigments used to drive many important biological processes. As a result, numerous artificial porphyrin-based arrays have been synthesised as bio-inspired electron-transfer reagents. Of particular importance have been the many dimeric porphyrins intended to mimic the 'special pair' that acts as primary electron donor in the photosynthetic bacterial reaction centre complex.[33] For such analogues,

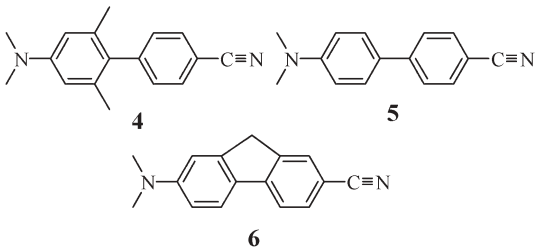

Fig. 13 Examples of twisted donor–acceptor biphenyls used to study how conformational relaxation is linked to electron transfer.

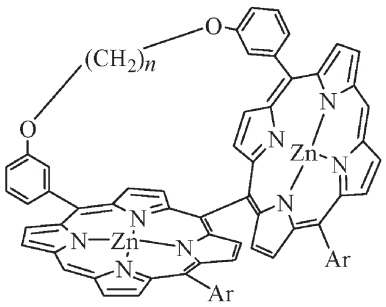

P(*n*)

Fig. 14 Examples of constrained porphyrin-based assemblies in which *n* varies from 2 to 10.

tuning and optimisation of electron transfer is achievable by altering the interporphyrin distance, electronic properties of the bridge, and the molecular orientation. Whilst the two former factors have been studied widely, the orientation effect is much less understood. In a recent study, Osuka and co-workers[34] have prepared a series of *meso–meso* linked Zn(II) bis-porphyrins **P(*n*)** (Fig. 14) to address this problem. For these bis-porphyrin compounds the available *n* values were 1–6, 8, and 10. As the length of the strap is shortened the dihedral angle between the rings decreases progressively (*e.g.*, **P6** 79°, **P1** 36°), and is accompanied by an increased distortion of the bis-porphyrin chromophore. For the case of **P(*n*)**, the fluorescence lifetimes gradually become shorter (1.96–1.53 ns) as the strap length decreases, indicating that structural distortions do not, to any significant extent, affect the emitting singlet state. That the strained compound **P2** exits in two conformers is supported by dual fluorescence, with conformer A exhibiting short wavelength emission (660 nm) and conformer B fluorescing in the near-infrared. Pronounced effects of changes in dihedral angle are seen in the absorption spectra of **P(*n*)**. As the strap length shortens, the intensity of the split Soret bands decreases and the Q-bands become split. Other optical spectroscopic measurements, such as circular dichroism and resonance Raman, display alterations that depend on the dihedral angle. It is evident from these preliminary studies that the approach used here to distort the bis-porphyrin geometry can provide a rather simple means by which to modify the properties of these chromophores. It will be interesting to see if similar variations can be imposed on the electronic properties.

10. Rigid molecular systems

Early research showed that the rates of through-bond electron transfer and electron exchange depend on the stereochemistry of the bridging unit.[35–37] It was found, in general, that trans orientations give higher rates than the corresponding cis geometries. Such conclusions tend to augment EPR studies made with organic biradicals in solution and frozen media.[38] A similar effect has been reported for donor–acceptor dyads linked *via* a σ-bond.[39,40] Interesting behaviour can be observed from the occurrence of slowly interconverting conformers in such systems, where solvent polarity plays a major role in defining the charge-transfer properties.

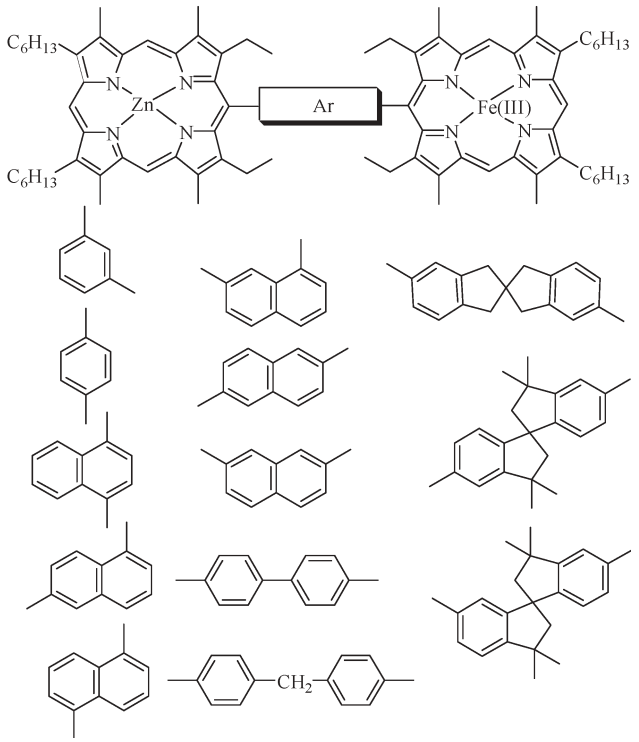

Fig. 15 Examples of the mixed-metal bis-porphyrins used to probe the distance and orientation effects on the dynamics of electron transfer.

Mataga and co-workers[41] showed that the rate of charge separation depends markedly on the separation distance but is relatively insensitive to the site of attachment for a series of zinc(II)/iron(III) mixed-metal bis-porphyrins (Fig. 15). The rate of the corresponding charge-recombination step was found to be independent of both separation distance and the site of attachment. Across the series of compounds, the attenuation factor β has a value of *ca.* 0.4 $Å^{-1}$.

Bocian *et al.*[42] have reported that the geometry of the bridge affects the rate of intramolecular electronic energy transfer in a series of bis-porphyrins (Fig. 16). Here, the rate constant for singlet energy transfer (k_{ENT}) decreases with increasing number of blocking groups added to the connecting phenylene rings. Thus, k_{ENT} decreases from $(24\ ps)^{-1}$ for the unhindered system, to $(46\ ps)^{-1}$ for the mono-hindered, to $(88\ ps)^{-1}$ for the bis-hindered derivative. The centre-to-centre separation remains at *ca.* 20 Å throughout the series and there are no obvious changes in thermodynamic properties. The blocking group has the effect of forcing that particular phenylene ring into an orthogonal geometry.

As mentioned earlier, McLendon *et al.*[16] observed that the rate of intramolecular electron transfer showed a precise relationship with the torsion angle around the connecting bond for the bis-porphyrins shown in Fig. 17. The minimum rate was found for angles around 45°, although it has to be stressed that the approach used will cause significant changes in the electronic properties of the biphenyl bridge. The results follow a rough "$\cos^2(2\theta)$" function, where θ is the torsion angle. There is no obvious reason for the coupling element being at a minimum around 45° and it will be interesting to see if the tethered strap approach pioneered by Benniston[22] will give a

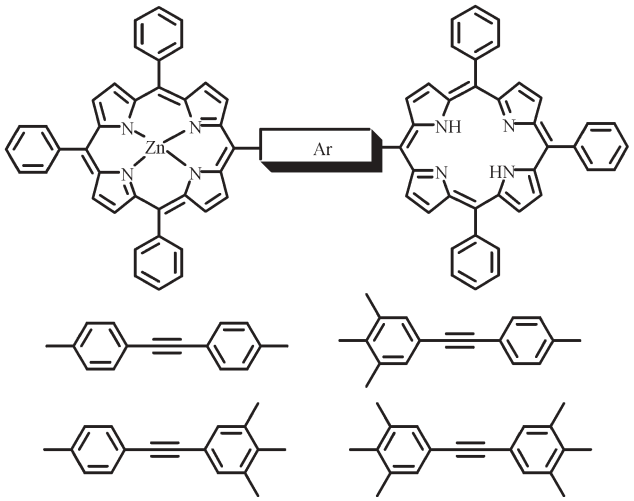

Fig. 16 Examples of the hindered bis-porphyrins used to probe orientation effects on the rates of electronic energy transfer.

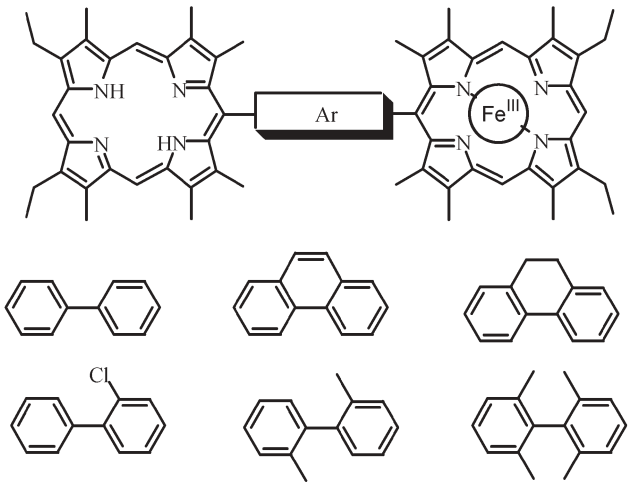

Fig. 17 Examples of the bis-porphyrins used to examine how the central torsion angle affects the rate of intramolecular electron transfer.

similar relationship. Of course, it is possible that the electronic properties of both donor and acceptor should be taken into account. In particular, it might be necessary to allow for different orbital symmetries and to consider how orbital nodes localised on donor and on the bridge interact. The metal poly(pyridine) complexes studied by Benniston push charge along the molecular axis, at least at the triplet level, and these might operate in a quite different way to the porphyrins used by McLendon.

11. Through-space interactions

An alternative to through-bond coupling is to employ systems where electron or energy transfer occurs by way of through-space interactions. Such interactions are especially important for electronic energy transfer involving singlet excited states where the Förster mechanism facilitates energy transfer over relatively large distances. Clearly, the propensity for through-bond or through-space electron transfer depends on the shape of the molecule and, in particular, on the mutual orientation of the reacting subunits. Molecular dyads built around highly flexible bridges can adopt "face-to-face" orientations that favour fast electron transfer. This is a well established strategy for promoting excimer or exciplex fluorescence. Equipping the molecule with some type of cavity allows the conformation to be switched by cation binding.[43] This allows fine control of the electron-transfer dynamics. Likewise, several molecular dyads have been designed where the through-space distance is much smaller than the shortest pathway along the bonding framework. Even so, electron transfer seems to prefer the longer through-bond route.

Positioning the electron-transfer partners at different sites along a polypeptide provides a simple way to vary their mutual orientation.[44] A somewhat more systematic approach has been introduced by Sakata *et al.*[45] Thus, a series of porphyrin-quinone dyads has been synthesised in which the orientation between porphyrin and quinone planes has been controlled (Fig. 18). The rates of electron transfer show a marked dependence on the orientation, although the thermodynamic driving force is fixed.

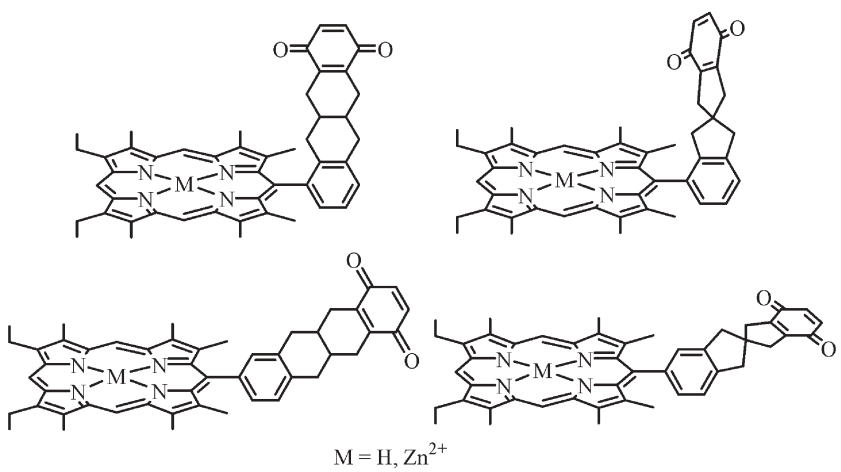

Fig. 18 Examples of porphyrin–quinone dyads exhibiting different mutual orientations.

12. Future prospects

It is apparent from several diverse experimental and theoretical studies that the rate of through-bond electron transfer depends on orientation factors. This applies both to the mutual orientation of the reactants and to geometric facets of the bridge itself. Perhaps the neatest aspect of this work relates to directing electron transfer through a biphenyl linker whose central torsion angle can be changed in a systematic way. Research has shown that the rate can be varied over a factor of about 80-fold by moving from coplanar to orthogonal structures. Adding two or more tethered biphenyls to the bridge is an obvious way to increase selectivity. This should be sufficient to achieve modest degrees of selectivity for sending an electron along one particular pathway when several identical paths are available. However, this approach requires the introduction of a means by which to alter the torsion angle in a reversible and controlled manner, rather than *via* the synthesis of discrete molecular bridges. Cation binding is one way to meet this challenge but, whilst being fully reversible, this is not an ideal methodology for rapid conformational switching. Other switching mechanisms based on optical or electrical stimulation are being actively considered.

One intriguing possibility to emerge from this research concerns the idea that the rates of charge separation (CS) and charge recombination (CR) might display different orientation effects. There are several hints that this might be the case. Thus, Mataga *et al.*[41] have shown that, at least in one case, CS and CR exhibit quite disparate distance dependencies. Bocian *et al.*[42] have reported that incorporating a phenylene spacer into the bridge has little effect on CS but causes a dramatic increase in the rate of CR. There appears to be a different angle dependence for hole transfer and electron delocalisation.[21] Finally, whereas McLendon *et al.*[16] find that the minimum rate of CS through a biphenyl spacer occurs at an angle of 45°, Benniston *et al.*[22] find that hole transfer is at a minimum when the torsion angle is 90°. If such systems could be optimised, it might be possible to extend the lifetimes of CS states by rapid switching of the torsion angle immediately after forward electron transfer has taken place. Again, there is a clear need to devise a satisfactory method for changing the conformation at will. This is now the key factor for the future development of smart materials that exploit orientation effects to achieve selective electron-transfer routes.

References

1 V. May and O. Kühn, *Charge and Energy Transfer Dynamics in Molecular Systems*, Wiley-VCH, Berlin, 2001.
2 J. J. Sumner and S. E. Creager, *J. Am. Chem. Soc.*, 2000, **122**, 11914.
3 I. Willner, *Acc. Chem. Res.*, 1997, **30**, 347.
4 R. A. Marcus and N. Sutin, *Biochim. Biophys. Acta*, 1985, **811**, 265.
5 J. R. Reimers, T. X. Lu, M. J. Crossley and N. S. Hush, *Nanotechnology*, 1996, **7**, 424.
6 N. Mataga, H. Chosrowjan and S. Taniguchi, *J. Photochem. Photobiol., C*, 2005, **6**, 37.
7 C. A. Naleway, L. A. Curtiss and J. R. Miller, *J. Phys. Chem.*, 1991, **95**, 8434.
8 N. P. Redmore, I. V. Rubtsov and M. J. Therien, *J. Am. Chem. Soc.*, 2003, **125**, 8769.
9 W. B. Davis, M. A. Ratner and M. R. Wasielewski, *J. Am. Chem. Soc.*, 2001, **123**, 7877.
10 R. H. Goldsmith, L. E. Sinks, R. F. Kelley, L. J. Betzen, W. Liu, E. A. Weiss, M. A. Ratner and M. R. Wasielewski, *Proc. Natl. Acad. Sci. U. S. A.*, 2005, **102**, 3540.
11 G. Pourtois, D. Beljonne, J. Cornil, M. A. Ratner and J. L. Bredas, *J. Am. Chem. Soc.*, 2002, **124**, 4436.
12 C. Lambert, G. Noll and J. Schelter, *Nat. Mater.*, 2002, **1**, 69; M. U. Winters, K. Pattersson, J. Martensson and B. Albinsson, *Chem.–Eur. J.*, 2005, **11**, 562.
13 J. R. Reimers and N. S. Hush, *Nanotechnology*, 1996, **7**, 417.
14 H. B. Gray and J. R. Winkler, *Proc. Natl. Acad. Sci. U. S. A.*, 2005, **102**, 3534.
15 H. M. McConnell, *J. Chem. Phys.*, 1961, **35**, 508.
16 A. Helms, D. Heiler and G. McLendon, *J. Am. Chem. Soc.*, 1991, **113**, 4325.
17 A. C. Benniston, A. Harriman, P. Y. Li and C. A. Sams, *Tetrahedron Lett.*, 2003, **44**, 4167.
18 A. C. Benniston, A. Harriman, P. Y. Li, C. A. Sams and M. D. Ward, *J. Am. Chem. Soc.*, 2004, **126**, 13630.
19 S. F. Nelsen, R. F. Ismagilov and D. A. Trieber, II, *Science*, 1997, **278**, 846.
20 J.-P. Launay, *Chem. Soc. Rev.*, 2001, **30**, 386.
21 A. C. Benniston, A. Harriman, P. Y. Li and C. A. Sams, *Phys. Chem. Chem. Phys.*, 2004, **6**, 875.
22 A. C. Benniston, A. Harriman, P. Y. Li and C. A. Sams, *J. Am. Chem. Soc.*, 2005, **127**, 2553.
23 D. H. Barich, R. J. Pugmire, D. M. Grant and R. J. Iuliucci, *J. Phys. Chem. A*, 2001, **105**, 6780.
24 W. M. Kwok, C. Ma, M. W. George, D. C. Grills, P. Matousek, A. W. Parker, D. Phillips, W. T. Toner and M. Towrie, *Phys. Chem. Chem. Phys.*, 2003, **5**, 1043.
25 I. Gomez, M. Reguero, M. Boggio-Pasqua and M. A. Robb, *J. Am. Chem. Soc.*, 2005, **127**, 7119.
26 D. Rappoport and F. Furche, *J. Am. Chem. Soc.*, 2004, **126**, 1277.
27 L. J. Charbonniere, R. Ziessel, C. A. Sams and A. Harriman, *Inorg. Chem.*, 2003, **42**, 3466.
28 J. Lappe, R. J. Cave, M. D. Newton and I. V. Rostov, *J. Phys. Chem. B*, 2005, **109**, 6610.
29 I. V. Rubtsov, N. P. Redmore, R. M. Hochstrasser and M. J. Therien, *J. Am. Chem. Soc.*, 2004, **126**, 2684.
30 G. Jones II, M. S. Farahat, S. R. Greenfield, D. J. Goztola and M. R. Wasielewski, *Chem. Phys. Lett.*, 1994, **229**, 40.
31 S. Fukuzumi, H. Kotani, K. Ohkubo, S. Ogo, N. V. Tkachenko and H. Lemmetyinen, *J. Am. Chem. Soc.*, 2004, **126**, 1600.
32 M. Maus, W. Rettig, D. Bonafoux and R. Lapouyade, *J. Phys. Chem. A*, 1999, **103**, 3388.
33 A. Harriman and J.-P. Sauvage, *Chem. Soc. Rev.*, 1996, **25**, 41.
34 H. S. Cho, J. K. Song, J. H. Ha, S. Cho, D. Kim and A. Osuka, *J. Phys. Chem. A*, 2003, **107**, 1897.
35 M. Antolovich, P. J. Keyte, A. M. Oliver, M. N. Paddon-Row, J. Kroon, J. W. Verhoeven, S. A. Jonker and J. M. Warman, *J. Phys. Chem.*, 1991, **95**, 1933.
36 B. P. Paulson, L. A. Curtiss, B. Bal, G. L. Closs and J. R. Miller, *J. Am. Chem. Soc.*, 1996, **118**, 378.
37 E. G. Petrov, I. S. Tolokhis, A. A. Demidenko and V. V. Gorbach, *Chem. Phys.*, 1995, **193**, 237.
38 M. D. E. Forbes, G. L. Closs, P. Calle and P. Gautam, *J. Phys. Chem.*, 1993, **97**, 3384.
39 J. Kurzawa, S. Schneider, J. Büber, R. Gleiter and T. Clark, *Phys. Chem. Chem. Phys.*, 2004, **6**, 3811.
40 P. P. Lainé, I. Ciofini, P. Ochsenbein, E. Amouyal, C. Adamo and F. Bedioui, *Chem.–Eur. J.*, 2005, **11**, 3711.
41 A. Osuka, K. Maruyama, N. Mataga, T. Asahi, I. Yamazaki and N. Tamai, *J. Am. Chem. Soc.*, 1990, **112**, 4958.
42 J. Seth, V. Palaniappan, R. W. Wagner, T. E. Johnson, J. S. Lindsey and D. F. Bocian, *J. Am. Chem. Soc.*, 1996, **118**, 11194.
43 A. Harriman, M. Hissler, P. Jost, G. Wippf and R. Ziessel, *J. Am. Chem. Soc.*, 1999, **121**, 14.
44 G. Jones, II, X. Zhou and V. I. Vullev, *Photochem. Photobiol. Sci.*, 2003, **2**, 1080.
45 Y. Sakata, H. Imhori, H. Tsue, S. Higashida, T. Akiyama, E. Yoshizawa, M. Aoki, K. Yamada, K. Hagiwara, S. Taniguchi and T. Okada, *Pure Appl. Chem.*, 1997, **69**, 1951.